On the Origin of High Ionic Conductivity in Na-doped $SrSiO_3$

Po-Hsiu Chien,[a] Youngseok Jee,[b] Chen Huang,[c] Riza Dervişoğlu,[d] Ivan Hung,[e] Zhehong Gan,[e] Kevin Huang[b] and Yan-Yan Hu*[ae]

[a]Department of Chemistry and Biochemistry, Florida State University, Tallahassee, FL 32306, USA
[b]Department of Mechanical Engineering, University of South Carolina, Columbia, SC 29208, USA
[c]Department of Scientific Computing, Florida State University, Tallahassee, FL 32306, USA
[d]Institute for Molecules and Materials, Radboud University, Nijmegen, AJ 6525, Netherland
[e]Center of Interdisciplinary Magnetic Resonance, National High Magnetic Field Laboratory, 1800 East Paul Dirac Drive, Tallahassee, FL 32310, USA

Table of Contents

1. Supporting Figures

1.1 ^{23}Na spectra of NaOH, SNS30, and β-$Na_2Si_2O_5$

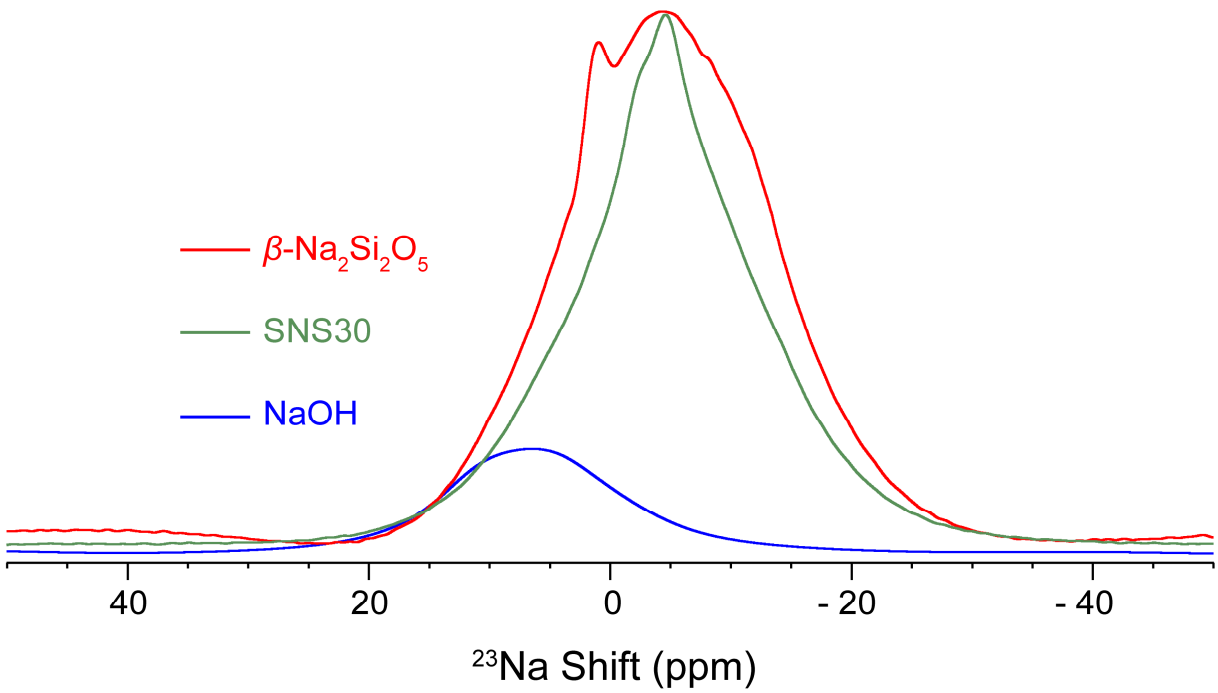

Figure S1. ^{23}Na spectra of NaOH (blue), SNS30 (green), and β-$Na_2Si_2O_5$ (red).

1.2 ^{17}O spectra of the SNS45 sample with and without ^{17}O-isotope enrichment

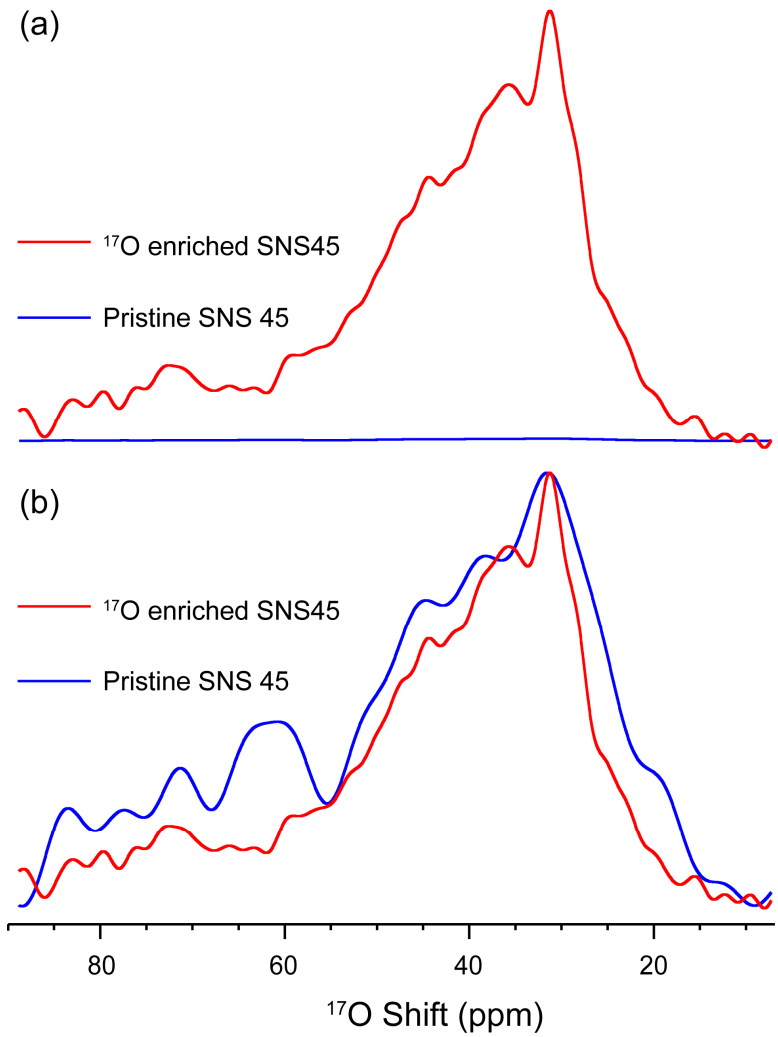

Figure S2. (a) Normalized ^{17}O spectra of the pristine SNS45 (blue) and the ^{17}O-enriched SNS45 (red); (b) ^{17}O spectra of the pristine SNS45 (scaled by 180-fold, blue) and the ^{17}O-enriched SNS45 (red).

1.3 Quantification of Chemical Species Found in SNS Samples

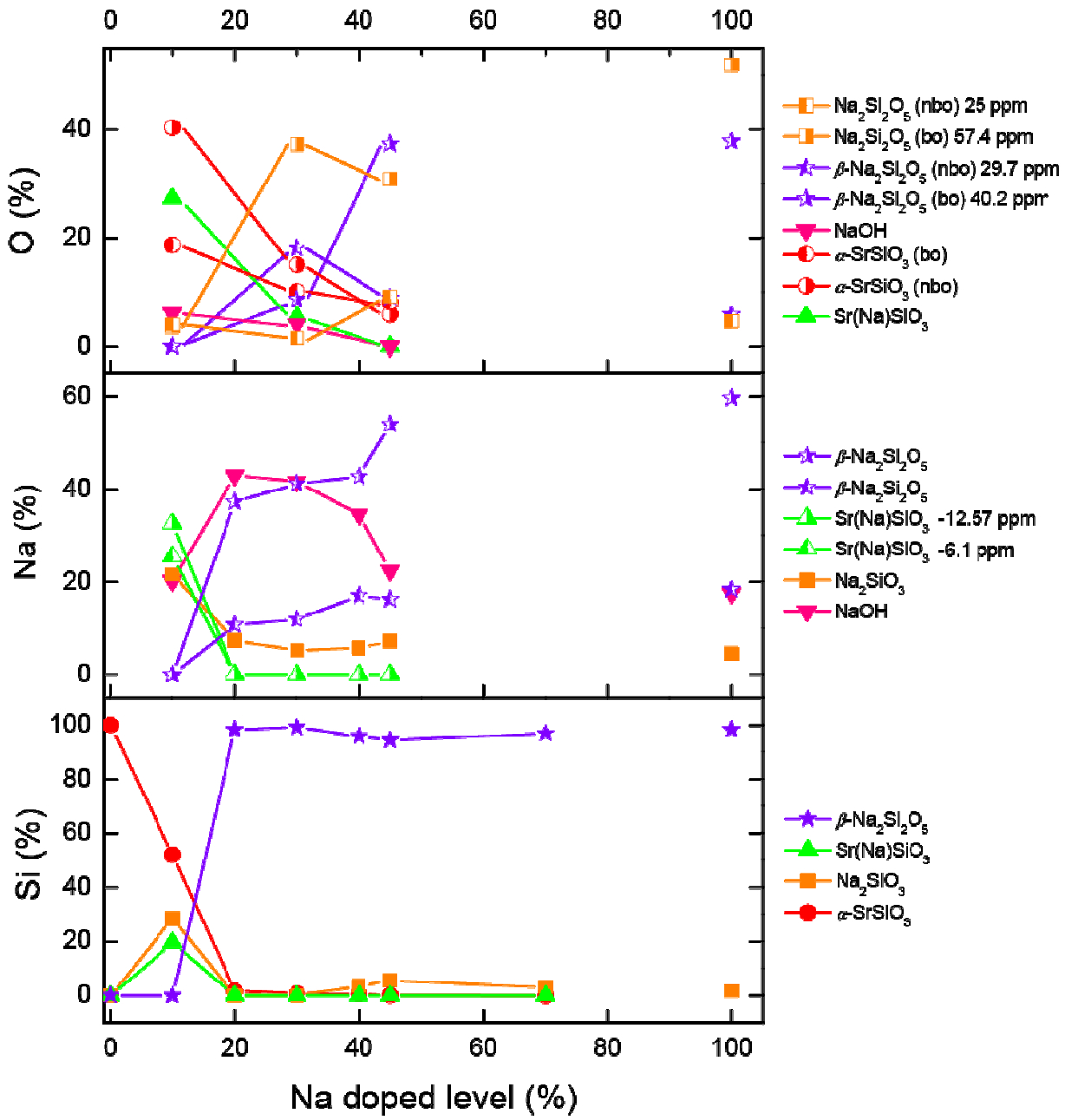

Figure S3. Quantification of Si, Na, and O in various chemical phases in SNS samples based on the area integral of the deconvoluted ^{29}Si, ^{23}Na, and ^{17}O NMR spectra in Figures 1, 2, and 3 in the main text.

1.4 Correlations between calculated ^{17}O isotropic shifts and Na – O bond distances in SNS40

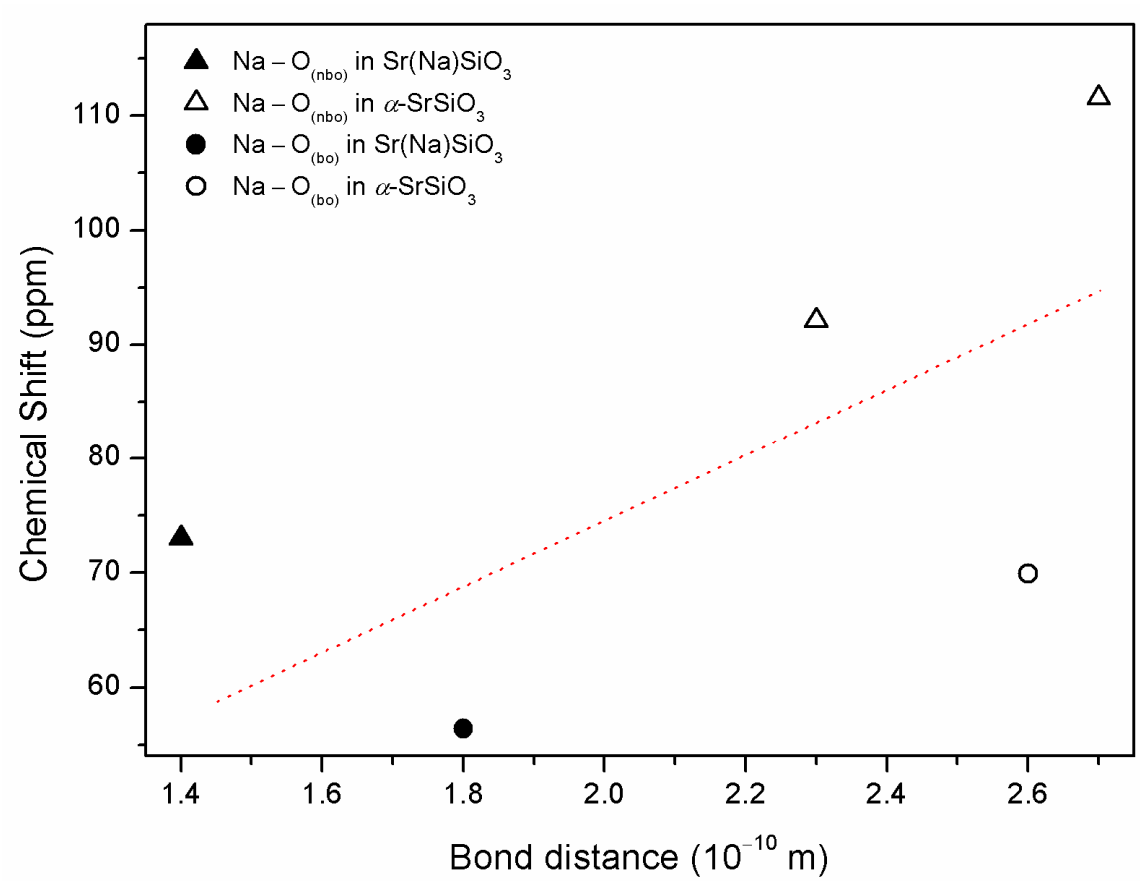

Figure S4. Plot of correlations between calculated ^{17}O isotropic shifts and (Na – O) bond distance in SNS40. Red dotted line is merely to guide the eyes.

The NMR calculations based on the ND structure reveals that the local environments of Si and O are very similar to those in α-$SrSiO_3$. Since the ND preferentially reveals long-range structural arrangement of crystalline phases; therefore, it is not surprising that the major phase β-$Na_2Si_2O_5$ in SNS40 is not captured in ND due to structural disorder. DFT calculations also show that for O sites near Na ions (effective Na–O distance < 2 Å) in the ND structure, the calculated ^{17}O isotropic resonances consistently shift to higher field (lower ppm) compared with those O sites far from Na ions (Fig. S4, Table S8).

2. NMR parameters derived from deconvolution of ^{29}Si, ^{23}Na, and ^{17}O spectra in Figures 1, 2, and 3

Table S1. ^{29}Si NMR of different Si sites in all the samples studied in this paper

Samples	Parameters	Components			
		α-$SrSiO_3$	Na_2SiO_3	$Sr(Na)SiO_3$	β-$Na_2Si_2O_5$
SNS 0	$\delta_{(iso)}$	-85.2	N/A	N/A	N/A
	LB	40.2	N/A	N/A	N/A
SNS 10	$\delta_{(iso)}$	-85.1	-76.7	-84.1	N/A
	LB	66.2	290.3	932.9	N/A
SNS 20	$\delta_{(iso)}$	-85.1	N/A	N/A	-88.5
	LB	39.2	N/A	N/A	812.8
SNS 30	$\delta_{(iso)}$	-85.2	N/A	N/A	-88.7
	LB	57.6	N/A	N/A	719.5
SNS 40	$\delta_{(iso)}$	-85.3	-78.0	N/A	-88.5
	LB	61.6	318.4	N/A	668.2
SNS 45	$\delta_{(iso)}$	-86.4	-78.0	N/A	-88.5
	LB	38.8	318.4	N/A	653.8
SNS 70	$\delta_{(iso)}$	N/A	-77.5	N/A	-88.8
	LB	N/A	318.4	N/A	677.6
β-$Na_2Si_2O_5$	$\delta_{(iso)}$	N/A	-77.2	N/A	-88.9
	LB	N/A	251.6	N/A	620.5

LB = line broadening factor

Table S2. ^{23}Na NMR of different Na sites in all the samples studied in this paper

Samples	Parameters	Components			
		NaOH	Na_2SiO_3	$Sr(Na)SiO_3$	
SNS 10	$\delta_{(iso)}$	7.9	-1.1	-6.1	-12.6
	C_Q (MHz)	3.5	2.0	1.8	0.47
	ε	0.79	0.93	0.32	0.03
	LB	1041.2	177.1	920.3	1669.7
		NaOH	Na_2SiO_3	β-$Na_2Si_2O_5$	
SNS 20	$\delta_{(iso)}$	5.7	-1.7	-5.3	-6.1
	C_Q (MHz)	3.3	2.0	1.9	3.5
	ε	1.00	0.98	0.03	0.03
	LB	1434.8	257.1	719.3	1129.8
SNS 30	$\delta_{(iso)}$	6.8	-2.2	-5.8	-4.7
	C_Q (MHz)	3.6	2.0	1.9	3.4
	ε	1.00	0.98	0.15	1.00
	LB	1094.8	257.1	619.3	1163.9
SNS 40	$\delta_{(iso)}$	8.9	1.6	-2.8	-4.3
	C_Q (MHz)	3.6	2.0	2.6	3.4
	ε	1.00	0.98	0.77	1.00
	LB	1098.6	266.2	389.3	1175.4
SNS 45	$\delta_{(iso)}$	11.1	2.0	-2.7	-2.0
	C_Q (MHz)	3.7	2.2	2.6	3.5
	ε	0.36	0.68	0.78	1.00
	LB	1113.0	68.4	398.46	1244
β-$Na_2Si_2O_5$	$\delta_{(iso)}$	10.8	2.5	-1.7	1.5
	C_Q (MHz)	3.2	2.0	2.4	4.3
	ε	1.00	0.61	0.19	0.63
	LB	753.8	133.4	1209.9	626.1

LB = line broadening factor

Table S3. ^{17}O NMR of different O sites in all the samples studied in this paper

Samples	Parameters	Components							
		$SrSiO_3$ (nbo)	$SrSiO_3$ (bo)	$Sr(Na)SiO_3$	NaOH	Na_2SiO_3 (bo)	Na_2SiO_3 (nbo)		
SNS 10	$\delta_{(iso)}$	109.2	80.1	126.3	66.5	72.0	38.5		
	C_Q (MHz)	2.8	4.0	0	8.3	4.7	2.3		
	ε	0.53	0.14	0.10	0.08	0.86	0.61		
	LB	434.8	204.4	8500.0	189.9	159.0	306.1		
						$Na_2Si_2O_5$ (bo)	$Na_2Si_2O_5$ (bo)	$Na_2Si_2O_5$ (nbo)	$Na_2Si_2O_5$ (nbo)
SNS 30	$\delta_{(iso)}$	108.8	80.3	101.2	67.2	62.9	47.1	40.2	39.2
	C_Q (MHz)	2.8	4.4	0	8.4	4.5	2.7	3.3	2.1
	ε	0.01	0.22	0.10	0.08	0.91	0.16	1.00	0.87
	LB	409.6	199.1	2484.0	57.9	289.0	400.0	0	60.9
SNS 45	$\delta_{(iso)}$	104.2	73.7	N/A	N/A	58.2	41.2	29.7	25.0
	C_Q (MHz)	2.9	4.1	N/A	N/A	5.0	4.0	2.1	2.3
	ε	0.53	0.27	N/A	N/A	0.78	0.66	0.43	0.54
	LB	434.8	126.8	N/A	N/A	159.6	327.3	127.4	88.6
β-$Na_2Si_2O_5$	$\delta_{(iso)}$	N/A	N/A	N/A	N/A	57.4	40.2	29.7	25
	C_Q (MHz)	N/A	N/A	N/A	N/A	5.1	3.9	2.4	2.3
	ε	N/A	N/A	N/A	N/A	0.54	0.71	0.20	0.33
	LB	N/A	N/A	N/A	N/A	297.2	359.5	119	138.1

LB = line broadening factor; bo = bridging oxygen; nbo = non-bridging oxygen; samples were all ^{17}O enriched, except for β-$Na_2Si_2O_5$

3. NMR quantification results of various chemical environments based on the deconvolution of ^{29}Si, ^{23}Na, and ^{17}O spectra in Figures 1, 2, and 3

Table S4. ^{29}Si quantification results of different Si sites in all the samples studied in this paper

Sample		Quantification			
		α-$SrSiO_3$	$Sr(Na)SiO_3$	β-$Na_2Si_2O_5$	Na_2SiO_3
SNS 0	Q	100.0	0	0	0
SNS 10	Q	52.1	19.5	0	28.5
SNS 20	Q	1.7	0	98.3	0
SNS 30	Q	0.7	0	99.3	0
SNS 40	Q	0.6	0	95.9	3.5
SNS 45	Q	0.1	0	94.4	5.5
SNS 70	Q	0	0	96.9	3.1
β-$Na_2Si_2O_5$	Q	0	0	98.3	1.7

Q = Quantity (%)

Table S5. ^{23}Na quantification results of different Na sites in all the samples studied in this paper

Sample		Quantification			
		NaOH	$Sr(Na)SiO_3$		Na_2SiO_3
SNS 10	Q	20.2	25.5	32.6	20.2
		NaOH	β-$Na_2Si_2O_5$		Na_2SiO_3
SNS 20	Q	43.8	10.9	37.8	7.5
SNS 30	Q	41.7	11.9	41.2	5.2
SNS 40	Q	34.5	17.1	42.7	5.8
SNS 45	Q	22.5	16.3	54.0	7.2
β-$Na_2Si_2O_5$	Q	17.6	18.3	59.6	4.5

Q = Quantity (%)

Table S6. ^{17}O quantification results of different O sites in all the samples studied in this paper

Samples		Quantification							
		$SrSiO_3$ (nbo)	$SrSiO_3$ (bo)	$Sr(Na)SiO_3$	NaOH	Na_2SiO_3 (bo)	Na_2SiO_3 (nbo)		
SNS 10	Q	40.6	18.8	27.3	6.1	3.6	4.0		
						$Na_2Si_2O_5$ (bo)	$Na_2Si_2O_5$ (bo)	$Na_2Si_2O_5$ (nbo)	$Na_2Si_2O_5$ (nbo)
SNS 30	Q	15.0	10.1	5.6	4.1	37.2	8.6	18.1	1.4
SNS 45	Q	5.8	8.0	N/A	N/A	30.8	37.3	8.9	9.1
β-$Na_2Si_2O_5$	Q	N/A	N/A	N/A	N/A	51.9	37.8	5.8	4.5

Q = Quantity (%); A = Absolute value

4. MQMAS fitting results

Table S7. ^{17}O quadrupolar interaction parameters of ^{17}O-enriched SNS45

Parameters			
Slice	Component	C_Q (MHz)	η
a	β-$Na_2Si_2O_5$ (nbo, red)	2.5	0.13
b	β-$Na_2Si_2O_5$ (nbo, green)	2.8	0.48
	β-$Na_2Si_2O_5$ (nbo, red)	2.5	0.13
c	Na_2SiO_3 (nbo, purple)	2.5	0.48
	β-$Na_2Si_2O_5$ (bo, navy blue)	4.5	0.88
d	β-$Na_2Si_2O_5$ (bo, navy blue)	4.5	0.88
e	β-$Na_2Si_2O_5$ (bo, dodge blue)	4.1	0.82
	β-$Na_2Si_2O_5$ (bo, violet red)	5.2	0.42
f	β-Na_2SiO_3 (bo, dark red)	5.1	0.49

5. First Principles DFT NMR Calculations

First principles solid-state electronic structure Density Functional Theory (DFT) NMR calculations were performed with the VASP (Vienna Ab initio Simulation Package) code.[1] Perdew-Burke-Ernzerhof revised for solids (PBEsol) was used.[2] Full structural optimizations including cell relaxations were carried out before NMR calculations. For structural optimization, a k-point mesh of 4 × 4 × 4 was used. The kinetic energy cut-off for the plane wave basis set was set to be 875 eV for full geometry relaxation (including cell relaxation), and was set to 600 eV for NMR. Gaussian smearing was applied with a smearing temperature of 0.01 eV. For NMR calculations, PBE generalized gradient approximation was employed.[3] A k-point mesh of 4 × 4 × 4 was used. The isotropic shielding was obtained as $\sigma_{\mathrm{iso}} = (\sigma_{xx} + \sigma_{yy} + \sigma_{zz})/3$ where σ_{xx}, σ_{yy}, and σ_{zz} are the principal components of the shielding tensor and $|\sigma_{zz} - \sigma_{iso}| \geq |\sigma_{xx} - \sigma_{iso}| \geq |\sigma_{yy} - \sigma_{iso}|$. The isotropic shift was calculated by the following equation: $\delta_{iso} = -[\sigma_{iso} - \sigma_{ref}]$ where the isotropic shielding of the system of interest and the reference system are σ_{iso} and σ_{ref}, respectively. NMR quadrupolar coupling parameters were defined as the following: quadrupolar coupling constant, $C_{\mathrm{Q}} = eQV_{zz}/h$; asymmetric parameter, $\eta_q = (V_{xx} - V_{yy})/V_{zz}$, where the electric field gradients tensors of the principal components $|V_{zz}| \geq |V_{yy}| \geq |V_{xx}|$.

First principles solid-state electronic structure Density Functional Theory (DFT) NMR calculations were performed with the Vienna Ab initio Simulation Package (VASP) on optimized structures of β-$Na_2Si_2O_5$ and SNS40 (apparent composition $Sr_{0.6}Na_{0.4}SiO_{2.8}$). The calculated NMR parameters are listed in table S8. The calculated parameters for ^{29}Si (shift), ^{23}Na (shift and C_{Q}), and ^{17}O (shift and C_{Q}) NMR of β-$Na_2Si_2O_5$ are consistent with reported theoretical and experimental results.[21] The consistency between calculated and experimental data validates the computational method employed here. With this validation, we have also predicted

NMR parameters for SNS40. The initial structure used in the calculation is from the neutron diffraction data (ND).[3] Geometry optimization was performed before NMR calculations.

Table S8. Calculated ^{29}Si, ^{23}Na, and ^{17}O NMR Parameters

Sample	element	δ_{iso} (ppm)	C_Q (MHz)
β-$Na_2Si_2O_5$	Na(1)	14.0	2.20
	Na(1)	7.9	2.19
	Si(1)	-87.0	N/A
	Si(2)	-85.3	N/A
	O (bo, 1)	58.0	5.21
	O (bo, 2)	54.9	5.32
	O (bo, 3)	56.3	5.22
	O (nbo, 1)	26.7	3.04
	O (nbo, 2)	30.4	2.73
$Sr_{0.6}Na_{0.4}SiO_{2.8}$	Na(1)	14.0	1.89
	Na(2)	8.5	1.61
	Si(1)	-88.5	N/A
	Si(2)	-85.1	N/A
	O (nbo, 1)	116.6	2.80
	O (nbo, 2)	92.1	3.03
	*O (nbo, 3)	73.0	3.01
	O (bo, 4)	69.9	4.77
	*O (bo, 5)	56.4	4.79

*O close to Na

6. Limitation of PFG NMR for reliably determining the Na ion diffusivity in SNS

The Nernst-Einstein equation provides the correlation between the ionic conductivity (σ/S cm^{-1}) and ion diffusivity (D/cm^2 s^{-1}) as

$$\boldsymbol{\sigma = Z^2F^2DC/RT} \qquad \text{(Eqn. S1)}$$

Z: the charge of Na^+, which is 1

F: Faraday constant, 9.648 x 10^4 C mol^{-1}

C: concentration of the charge carrier, i.e. Na^+

R: gas constant, 8.314 J K^{-1} mol^{-1}

T: temperature, K

With the highest conductivity measured in the Na-doped $SrSiO_3$ sample,[4] i.e., 10^{-2} S cm^{-1} at 525 ^{o}C and a reasonable assumption that Na^+ is the only charge carrier in this sample, the estimated diffusivity is 10^{-7} S cm^{-1}. At temperatures < 400 ^{o}C, the measured conductivity is < 10^{-3} S cm^{-1}, which corresponds to a Na^+ diffusivity smaller than 10^{-8} S cm^{-1}.

Most PFG NMR measurements were carried out to study gas or ions in liquids diffusing through porous media,[5–6] which possess significantly faster diffusion compared with ion diffusion in solids. We could evaluate the practicality of measuring the Na^+ diffusivity using PFG measurements through the following calculations. In PFG experiments, the diffusivity coefficient is determined via a spin-echo attenuation of the following exponential form

$$S_{(q,t)} = S_{(q,0)} \exp(-q^2Dt) \qquad \text{(Eqn. S2)}$$

$S_{(q,t)}$: echo intensity after diffusion time interval t

$S_{(q,0)}$: echo intensity at time origin, no diffusion

q: scattering wave-number

$$q = \gamma\, \delta\, g$$

(γ: gyromagnetic ratio of the nucleus, δ: width of the field gradient pulses, g: strength of the field gradient)

As a prerequisite for a reliable measurement of the signal attenuation given by the equation S2, the exponent q^2Dt has to be on the order of or larger than 1. With a typical maximum values of g = 30 T m^{-1}, δ = 2 ms, and γ (^{23}Na) = 7.076×10^7 T^{-1} s^{-1}, the mean value of the molecular displacements is found to be on the order of hundreds of nm. With the fast relaxation of ^{23}Na resonances as measured by Dr. I. Evans' group,[7] i.e., T_1, on the order of a few ms, the minimum diffusivity measurable by ^{23}Na PFG NMR is 10^{-6} – 10^{-7} cm^2 s^{-1}. Based on our survey of the literature on ^{23}Na PFG experiments, the lowest diffusivity measured is on the order of 10^{-6} cm^2 s^{-1} in solution/lipids.[8–9]

Based on the analysis above, the Na ion diffusivity (10^{-7} – 10^{-8} cm^2 s^{-1}) in the Na-doped $SrSiO_3$ sample is estimated to be below the detection limit (10^{-6} – 10^{-7} cm^2 s^{-1}) of ^{23}Na PFG NMR at the state-of-the-art. The rapid relaxation of ^{23}Na resonance is the main limiting factor.

Reference:

1. P. E. Blöchl, O. Jepsen and O. K. Andersen, *Phys. Rev. B*, 1994, **49**, 16223.
2. J. P. Perdew, A. Ruzsinszky, G. I. Csonka, O. A. Vydrov, G. E. Scuseria, L. A. Constantin, X. Zhou and K. Burke, *Phys. Rev. Lett.*, 2008, **100**, 136406-1.
3. J. P. Perdew, K. Burke and M. Ernzerhof, *Phys. Rev. Lett.*, 1996, **77**, 3865.
4. P. Singh and J. B. Goodenough, *J. Am. Chem. Soc.*, 2013, **135**, 10149.
5. J. Kärger and R. Valiullin, *Chem. Soc. Rev.*, 2013, **42**, 4172.
6. S. Beckert, F. Stallmach, H. Toufar, D. Freude, J. Kärger and J. Haase, *J. Phys. Chem. C*, 2013, **117**, 24866.
7. J. R. Peet, C. M. Widdifield, D. C. Apperley, P. Hodgkinson, M. R. Johnson and I. R. Evans, *Chem. Commun.*, 2015, **51**, 17163.
8. Y. Wang, J. Gao, T. J. Dingemans and L. A. Madsen, *Macromolecules*, 2014, **47**, 2984.
9. K. I. Momot, P. W. Kuchel and D. Whittaker, *Langmuir*, 2004, **20**, 2660.